

Covalent Heme Framework as a Highly Active Heterogeneous Biomimetic Oxidation Catalyst

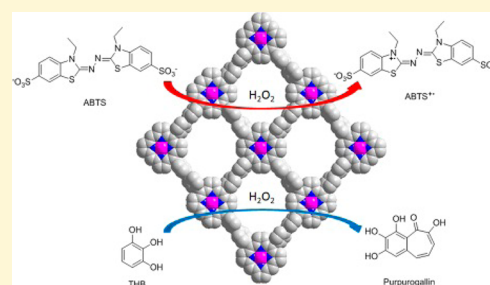
Xi-Sen Wang,[†] Matthew Chrzanowski,[†] Daqiang Yuan,[‡] Brandon S. Sweeting,[†] and Shengqian Ma^{*,†}

[†]Department of Chemistry, University of South Florida, 4202 East Fowler Avenue, Tampa, Florida 33620, United States

[‡]State Key Laboratory of Structural Chemistry, Fujian Institute of Research on the Structure of Matter, Chinese Academy of Sciences, Fujian, Fuzhou 350002, P. R. China

S Supporting Information

ABSTRACT: Although the active centers of many metalloenzymes have been well-studied, the ability for chemists to imitate the iron porphyrin heme found in these enzymes remains a challenge. Herein, we report a water/chemical-stable nanoporous covalent heme framework (CHF-1) that can be synthesized via the Yamamoto homocoupling reaction. Unlike other artificial enzymes, CHF-1 neatly arranges the heme centers to form a graphene-like two-dimensional framework bearing a high surface area (1620 m²/g) and high density of active sites. Biomimetic catalytic reactions show that CHF-1 catalyst is an effective heterogeneous catalyst with exceptionally high binding affinities and high catalytic efficiency approaching that of natural heme-based enzymes.



INTRODUCTION

Cytochrome P450, an enzyme found ubiquitously throughout the natural world in all domains of life, functions as a mono-oxygenase that carries out various detoxification processes in biosynthetic pathways.¹ Its active site contains an Fe(III) porphyrin heme complex (Figure 1a) that can reversibly bind

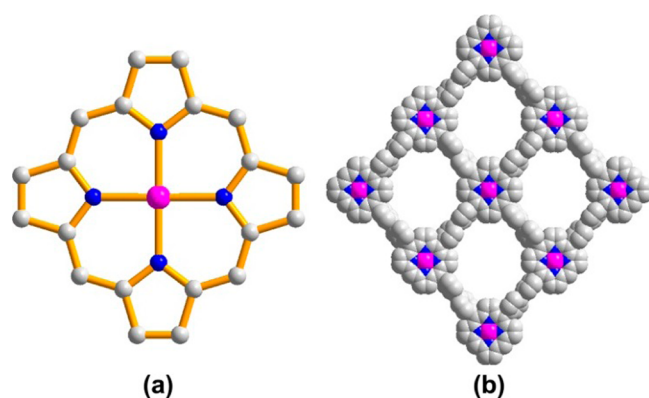


Figure 1. Structures of (a) iron porphyrin (heme) and (b) microporous iron(III) porphyrin framework CHF-1.

oxygen through its iron ion, which acts as an oxygen carrier. The heme complex can also transport electrons by changing the oxidation state of the iron ions, thus concurrently acting as an electron carrier.² Using this efficient natural catalyst as a blueprint, many artificial systems containing heme active centers (iron(III) porphyrins) have been developed³ and used in biomimetic catalytic reactions.⁴ Iron porphyrins (Figure 1a), however, have been found to form catalytically inactive dimers easily in oxidizing reaction media.⁵ Nonetheless, several

successful strategies have been formulated to prevent the formation of inactive dimers. One such example involves loading iron porphyrins onto supports, but this unavoidably dilutes the density of the active sites.^{6,7} Another strategy decorates the porphyrin macrocycle with bulky functional groups to protect the iron porphyrin centers. This strategy, however, is limited by the difficulty of synthesizing these porphyrins.⁸ An additional strategy that has attracted escalating interest in recent years is to encapsulate heme into metal-organic frameworks (MOFs) directly^{9–12} or to use metalated porphyrin ligands to construct MOFs.^{13–19} Although MOFs demonstrate great potential in many fields,²⁰ such as gas storage,²¹ gas separation,²² carbon capture,²³ catalysis,²⁴ and others, water/chemical stability still remains an important issue to be addressed.²⁵ Moreover, a problem arises in the fact that the metal centers in the secondary building units (SBUs) of MOFs have been shown to be catalytically active Lewis acid catalysts.^{12,15,19} The activity in these metal centers could confound the mimicking of the catalytic processes of the hemes.¹⁹ Therefore, there is still an urgent need for developing new types of materials that are water/chemical-stable as well as have high catalytic activity and distinct substrate selectivity that mimic natural enzyme reactions.

Over the past several years, there has been an increasing interest in the study of porous organic polymers. Their exceptionally high surface areas, uniform yet tunable pore sizes, and high thermal/chemical/water stabilities make them promising for various applications, particularly for gas storage and CO₂ capture.^{26–48} The porous organic polymers are

Received: November 21, 2013

Revised: January 27, 2014

Published: February 11, 2014

typically composed of multitopic organic ligands linked by covalent bonds into two- or three-dimensional (2D or 3D) frameworks, resulting in framework structures that contribute no catalytic activity. When catalytically active monomers are employed, porous organic polymers become promising candidates as heterogeneous catalysts. The incorporation of iron porphyrin (heme) centers as monomers, although rarely explored, establishes heterogeneous biomimetic catalyst systems in the domain of porous organic polymers.^{45–48}

Most recently, a biomimetic catalyst was achieved by using graphene as a support, although the active centers (iron porphyrin) were randomly dispersed on the surface of the graphene.⁷ The porphyrin–graphene heterostructures, formed through π – π stacking, demonstrated excellent performance in biomimetic catalytic reactions. It can be envisioned that if the active centers can be neatly arranged to form a graphene-like 2D porous covalent organic framework bearing high surface areas and high density of active sites then this may provide an ideal system both to enhance the catalytic activity and to protect the active centers.

This challenge was addressed by directly incorporating heme (iron porphyrin) into a 2D covalent metalloporphyrin framework using a Yamamoto homocoupling reaction with a custom-designed porphyrin as the starting material.^{30–32} The resulting covalent heme framework not only stabilizes the heme by hindering it from forming catalytically inactive dimers but also allows the heme to be ordered into a 2D framework, thus resulting in high catalytic activity. Additionally, the afforded covalent heme framework features high thermal, chemical, and water stabilities, thus meeting all of the prerequisites for a biomimetic system. In this contribution, we report the construction of a porphyrin-based conjugated porous organic polymer utilizing the custom-designed porphyrin ligand, iron(III) meso-5,10,15,20-tetrakis(4-bromophenyl)porphyrin chloride (Fe(tbpp)Cl), as a building block. We hypothesize that the homocoupling of Fe(tbpp)Cl building blocks will lead to a 2D layered framework with the heme centers ordered on the surface, and the exposed iron porphyrin can render high biomimetic catalytic activity. As expected, the resultant material, named CHF-1 (CHF denotes covalent heme framework), possesses high water stability and exhibits near-enzyme-like activity in biocatalytic reactions.

RESULTS AND DISCUSSION

Preparation and Physicochemical Characterization of CHF-1. CHF-1 was synthesized by Yamamoto homocoupling reaction for polymerization, which has been proven to be efficient in synthesizing porous organic frameworks, such as PAFs and PPNs.^{30,31} Typically, to a solution of 2,2'-bipyridyl, bis(1,5-cyclooctadiene)-nickel(0) (Ni(COD)₂) and 1,5-cyclooctadiene (COD) in anhydrous DMF/1,4-dioxane was added iron(III) tetra(4-bromophenyl)porphyrin chloride, and the mixture was stirred at room temperature under an argon atmosphere overnight. After reaction, the mixture was cooled in an ice bath and a 50% acetic acid solution was added, and the resulting mixture was stirred for another night and then washed and dried in vacuum to give CHF-1 as a dark-red powder in 78% yield.

The polymer CHF-1 is a dark-gray powder that is insoluble in common organic solvents and resistant toward bases and weak acids. FTIR measurements show the disappearance of the C–Br vibration band in the spectra of CHF-1, confirming the completion of the coupling reactions. The powder X-ray

diffraction (PXRD) patterns indicate that CHF-1 is an amorphous polymer, although some overlap exists between the calculated PXRD patterns of the simulated structure and the experimental ones of CHF-1. TGA measurement shows CHF-1 possesses high thermal stability (Figure S1–S3 in the Supporting Information). Field-emission scanning electron microscopy (FE-SEM) images show that CHF-1 is composed of agglomerated ball-shaped particles with sizes ranging from 200 to 400 nm in diameter (Figure 2a), which indicates the roughness of its surface.

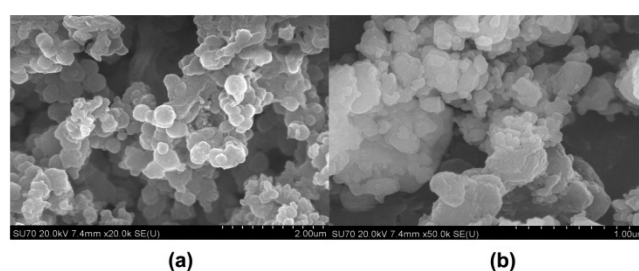


Figure 2. SEM image of (a) CHF-1 and (b) CHF-1 supported on BaSO₄.

The model of the possible structure of CHF-1 was simulated through Universal force-field calculations using the Focite Module in Accelrys' Materials Studio (MS) v. 6.1 software⁴⁹ (Figure 1b). On the basis of the PXRD patterns, gas-adsorption studies, and other similar structure simulations reported previously,^{32,45} the optimized simulation generated a structure with the *Pbcn* space group and a unit cell with $a = 22.7876 \text{ \AA}$, $b = 24.9077 \text{ \AA}$, and $c = 9.9249 \text{ \AA}$. The model indicated that the planar porphyrin rings and chair-form phenyl rings are connected to extend into wavelike sheets and that the sheets prefer ABAB stacking to form aligned tubular channels. To assess the permanent porosity of CHF-1, gas-sorption measurements were performed on the activated CHF-1 sample. The N₂ adsorption isotherm at 77 K revealed that CHF-1 exhibits an uptake capacity of 720 cm³/g at saturation pressure with typical type-I sorption behavior (Figure S4 in the Supporting Information), as expected for microporous materials. Derived from the N₂ adsorption data, CHF-1 has a BET surface area of 1620 m²/g ($P/P_0 = 0.02–0.2$). Density functional theory (DFT) pore-size distribution analysis based on the N₂ adsorption data at 77 K indicated that the pore size of CHF-1 is narrowly distributed around 7.0 Å, smaller than the pore size (~9 Å) of PCPF-1 with a AA packing structure,³² which also suggests a 2D layered structure with ABAB stacking for CHF-1 (Figure S4 in the Supporting Information).

Biocatalytic Properties of CHF-1. The ordered arrangement of hemes (iron(III) porphyrin macrocycles) with the five-coordinate iron(III) centers oriented on the surface of CHF-1 prompted us to evaluate the biocatalytic performance of CHF-1. The catalytic activity of CHF-1 was investigated by enzyme kinetics theory and methods using two reactions. The first (the oxidation reaction of 2,2'-azino-di(3-ethylbenzothiazoline)-6-sulfonate (ABTS) to ABTS^{•+}) involves electron transfer, whereas the second (the oxidation of pyrogallol to purpurogallin) necessitates oxygen transfer. These reactions are routinely used to evaluate the peroxidase activity of porphyrin catalysts. Control experiments were conducted using FeTPPCL and free-base CHF-1 under identical conditions. For comparison, experiments were also carried out for horse-radish

peroxidase (HRP) in the homogeneous system under similar conditions. Kinetic studies revealed that CHF-1 exhibited excellent peroxidase-like catalytic activity, better than that of the reported MOFs. To the best of our knowledge, CHF-1 is the first porous covalent polymer that is a heterogeneous biomimetic catalyst applied in biomimetic reactions.

To solve the issue of CHF-1 floating on the surface of water because of its low density, powder BaSO₄ was added and mixed with CHF-1 before catalytic assays. The concentration of the heme centers in the mixture material is about 2.12×10^{-4} mmol/mg, as obtained from ICP-MS experiments on the activated CHF-1 sample. The SEM image shows that the mixture material is composed of agglomerated ball-shaped particles with sizes ranging from 100–200 nm in diameter (Figure 2b). The reactions using BaSO₄ or free-base CHF-1 are very similar to the blank reaction, indicating that BaSO₄ and free-base CHF-1 are catalytically inactive (Figure S5 and S6 in the Supporting Information).

The catalytic activity of CHF-1 in the oxidation reaction of ABTS to ABTS^{•+} under the optimum conditions was investigated. The reaction progress was monitored by kinetic mode UV–vis spectroscopy at 660 nm with a particular range of ABTS concentration, which was consistent with typical Michaelis–Menten kinetics (Figure 3). To determine the effect of the pH value on the catalytic reaction, the initial rates of the same reaction in different pH values were tested in tris(hydroxymethyl)aminomethane (Tris) buffer solution, which was selected because of the favorable reaction conditions

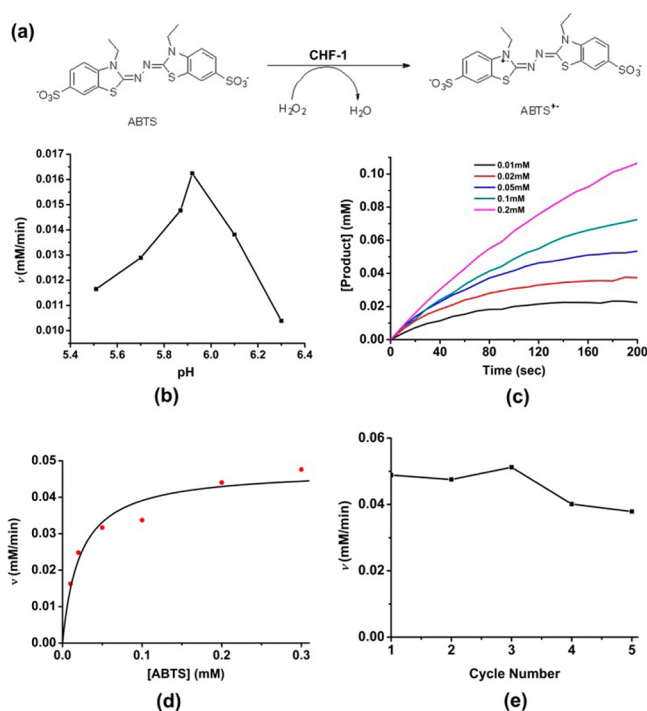


Figure 3. Oxidation reaction of ABTS catalyzed by CHF-1. (a) Oxidation reaction of ABTS in which ABTS is oxidized to ABTS^{•+} by H₂O₂. (b) Oxidation reaction of 0.1 mM ABTS catalyzed by CHF-1 at different pH values of the Tris buffer. (c) Initial ABTS oxidation profile catalyzed by CHF-1 (0.106 mM hemein equivalent). The concentrations of ABTS range from 0.01 to 0.2 mM. (d) Michaelis–Menten curve fit for the ABTS oxidation catalyzed by CHF-1. (e) Oxidation reaction of 0.1 mM ABTS catalyzed by CHF-1 at different cycles.

(Figure 3a). To gain better insight into this catalyst, control experiments were performed under similar catalytic reaction conditions using FeTPPCL and HRP but in homogeneous systems (Figure S7 in the Supporting Information). The maximum number of substrate molecules turned over per catalyst molecule per unit time (k_{cat}), the Michaelis–Menten constant (K_m) associated with the affinity of the catalyst molecules for the substrate, and the catalytic efficiency (k_{cat}/K_m) were obtained using a Michaelis–Menten curve fit, which is shown in Table 1. For the ABTS oxidation reaction, the derived k_{cat} of the CHF-1 catalyst shows a value of 0.45 min^{-1} . This value is less than that of FeTPPCL (3.67 min^{-1}) and HRP (887.54 min^{-1}). Additionally, the derived (K_m) value of the CHF-1 (0.022 mM) is four times higher than FeTPPCL (0.0055 mM), whereas it is about 1 order of magnitude lower than that of HRP (0.15 mM). Because the ABTS oxidation reaction over CHF-1 is heterogeneous (requiring substantial mass transfer over the heterogeneous phases, whereas the reaction using other catalysts are homogeneous), the affinity of CHF-1 for the ABTS is higher than that of the homogeneous catalyst FeTPPCL; nonetheless, the active centers in HRP, unlike those in the other homogeneous catalyst, FeTPPCL, are protected by the peptide chains, which create some barriers for the substrate to interact directly with the active centers. In a brief summary, the results of the measure of the catalytic efficiency indicated that the CHF-1 exhibits excellent catalytic efficiency ($k_{\text{cat}}/K_m \approx 2.06 \times 10^4 \text{ M}^{-1} \text{ min}^{-1}$), which approaches that of the natural enzyme HRP ($k_{\text{cat}}/K_m \approx 5.94 \times 10^6 \text{ M}^{-1} \text{ min}^{-1}$). Such an excellent electron-transfer catalytic performance can be attributed to the high density of the heme active centers in CHF-1, which facilitates the affinity for the substrate ABTS. To evaluate the recyclability of CHF-1, the heterogeneous catalyst was recovered for a further catalytic test of ABTS oxidation at different cycles with the initial rates being examined. The rate at the second cycle was $0.047 \mu\text{mol}/\text{min}$ (50 s), representing 97% of its initial activity. With the increasing number of cycles, the catalytic activity of CHF-1 gradually decreased, and at the fifth cycle, it could still retain ~80% of its initial catalytic activity (Figure 3d). Because there was no detectable leaching of active-site or Fe(III) ions in the supernatant of the reaction solution, the apparent decrease in activity could be attributed to the catalyst loss during the recovery procedure, as a small portion of catalyst was found on the wall of the centrifuge tube or glass pipet after each recovery. This recyclability validates the heterogeneous nature of the biomimetic catalysis by CHF-1.

We also assessed the catalytic activity of CHF-1 in the oxidation of pyrogallol to purpurogallin. The kinetic parameters of the Michaelis–Menten equation were determined for CHF-1. Experiments were carried out using different pyrogallol concentrations (0.01–0.2 mM) in 4-(2-hydroxyethyl)-1-piperazineethanesulfonic acid (HEPES) buffer (pH \approx 7.5). Catalytic studies of the pyrogallol oxidation reaction with CHF-1 show similar behavior to that in the oxidation reaction of ABTS to ABTS^{•+} (Figure 4). The Michaelis–Menten curve fit gives a k_{cat} value of 0.33 min^{-1} , lower than the recently reported k_{cat} of the porphyrin-based MOF PCN-222(Fe) (16.1 min^{-1}), both of which are heterogeneous catalysts (Table 1). Nonetheless, the K_m value of CHF-1 (0.0040 mM) was about 1 or 2 orders of magnitude lower than that of other catalysts, indicating very high affinity of CHF-1 for the substrate THB molecule. Although the k_{cat} value of other investigated catalysts showed higher results when compared to CHF-1, the catalytic efficiency

Table 1. Kinetic Parameters for the Oxidation of Substrates by Different Catalysts

| substrate | catalyst | k_{cat} (min^{-1}) | K_{m} (mM) | $k_{\text{cat}}/K_{\text{m}}$ ($\text{M}^{-1} \text{min}^{-1}$) |
|-----------|-------------------------------|--|---------------------|---|
| ABTS | CHF-1 | 0.45 3.67 | 0.022 | 2.06×10^4 |
| | FeTPPCL | 887.54 | 0.0055 | 6.62×10^5 |
| | HRP | 3.67 | 0.15 | 5.94×10^6 |
| THB | CHF-1 | 0.33 | 0.0040 | 8.26×10^4 |
| | HRP | 1965 | 0.89 | 2.2×10^6 |
| | hemin-graphene ⁷ | 246 | 1.22 | 2.0×10^5 |
| | FeTMPyP-graphene ⁷ | 545 | 0.96 | 5.7×10^5 |
| | PCN-222(Fe) ¹⁸ | 16.1 | 0.33 | 4.85×10^4 |

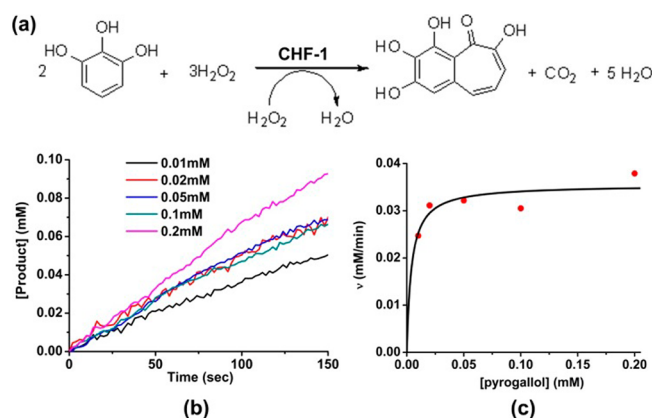


Figure 4. Oxidation reaction of pyrogallol catalyzed by CHF-1. (a) Oxidation reaction of pyrogallol in which pyrogallol is oxidized to purpurogallin by H_2O_2 . (b) Initial pyrogallol oxidation profile catalyzed by CHF-1 (0.106 mM hemin equivalent). The concentrations of pyrogallol range from 0.01 to 0.2 mM. (c) Michaelis–Menten curve fit for the pyrogallol oxidation catalyzed by CHF-1.

of the CHF-1 ($k_{\text{cat}}/K_{\text{m}} \approx 8.26 \times 10^4 \text{ M}^{-1} \text{ min}^{-1}$) is about two times as high as the recently reported porous heterogeneous catalyst PCN-222(Fe)¹⁸ ($k_{\text{cat}}/K_{\text{m}} \approx 4.85 \times 10^4 \text{ M}^{-1} \text{ min}^{-1}$) and is comparable with the catalytic efficiency of homogeneous catalysts, hemin-graphene ($k_{\text{cat}}/K_{\text{m}} \approx 2.0 \times 10^5 \text{ M}^{-1} \text{ min}^{-1}$)⁷ and FeTMPyP-graphene ($k_{\text{cat}}/K_{\text{m}} \approx 5.7 \times 10^5 \text{ M}^{-1} \text{ min}^{-1}$)⁷. Furthermore, the catalytic efficiency of CHF-1 approaches that of the natural enzyme HRP ($k_{\text{cat}}/K_{\text{m}} \approx 2.6 \times 10^6 \text{ M}^{-1} \text{ min}^{-1}$) (Figure S8 in the Supporting Information), which is consistent with that reported in the literature.⁷ From these results together with the results of the oxidation reaction of ABTS to ABTS^{•+}, it is very clear that the CHF-1 catalyst is an effective heterogeneous biomimetic catalyst with high catalytic efficiency approaching that of the natural enzyme.

DISCUSSION

All of these results demonstrate the feasibility of precisely designing a covalent heme framework for mimicking heme-based proteins applications. Clearly, designing a covalent framework or other material with a higher density of enzyme active centers will substantially improve the overall catalytic activity and catalytic efficiency in biomimetic reactions, such as the covalent heme framework (CHF-1) in the peroxidase-mimicking system presented herein. Heterogeneous artificial enzymes require the following four fundamental guidelines for the proposed materials: (1) a high density of active centers, (2) a complete lack of catalytic activity from the framework, (3) water/chemical/thermal stability, and (4) ease of recovery and recycling. Here, we present for the first time (to our knowledge) the design of a heme covalent polymer to address

the ability to mimic heme-based protein applications based on its chemical (active centers, etc.) and physical properties. Neatly arranging heme centers into 2D covalent organic frameworks improves the density of the active centers because the active centers are preloaded for specific biocatalytic reactions. Additionally, using heme centers as monomers for a covalent organic framework also simultaneously endows the material with specificity in mimicking protein reactions.

CONCLUSIONS

The enzyme active center has been utilized in designing porous covalent materials at the molecular level for biomimetic catalytic applications. As an experimental proof of concept, such a covalent framework was first designed and synthesized for biomimetic catalytic applications through the precise selection of heme derivative as monomer for polymerization. Experimental and structural simulation results demonstrate the high density of the active centers in the polymer and high catalytic efficiency of the heme covalent polymer as heterogeneous biomimetic catalyst, which approaches that of natural enzymes. Building the heme active centers into a porous organic polymer with an extended framework structure was achieved, again, through ligand design. This resulting covalent heme framework possesses a high density of active centers, resulting in high catalytic efficiency in biomimetic catalytic reactions. In principle, this work lays the foundation for the development of new covalent polymer and composite materials for biomimetic catalytic applications through the use of enzyme-like active centers as monomer building blocks.

EXPERIMENTAL SECTION

Materials and Syntheses. Commercially available reagents were purchased in high purity and used without further purification. Iron(III) meso-5,10,15,20-tetrakis(4-bromophenyl)porphyrin chloride (Fe(tbpp)Cl) was synthesized according to literature methods.⁴⁵ Solvents were purified according to standard methods and stored in the presence of molecular sieves. A microgram balance (TA Instrument TGA 2950 Hi-Res) was used to measure the mass of the catalyst.

Synthesis of CHF-1. A solution of 2,2'-bipyridyl (226 mg, 1.45 mmol), bis(1,5-cyclooctadiene)nickel(0) (Ni(COD)₂, 400.0 mg, 1.45 mmol), and 1,5-cyclooctadiene (COD, 0.18 mL, 1.46 mmol) in anhydrous DMF/1,4-dioxane (24.0 mL/36.0 mL) was added to iron(III) meso-5,10,15,20-tetrakis(4-bromophenyl)porphyrin chloride (326.0 mg, 0.32 mmol), and the mixture was stirred at room temperature under a nitrogen atmosphere overnight. Then, the mixture was cooled in an ice bath followed by the addition of a 50% acetic acid solution (20 mL), and the resulting mixture was stirred overnight. The precipitate was collected and washed with chloroform (6 × 10 mL), THF (6 × 10 mL), methanol (6 × 10 mL), and water (6 × 10 mL) and rigorously washed by Soxhlet extractions for 24 h with chloroform, THF, methanol, and acetone as solvent, respectively, dried

in vacuum and then dried under dynamic vacuum to afford CHF-1 as dark-red powder (175 mg, 0.25 mmol, 78%).

Gas Adsorption. Gas adsorption measurements were performed using an ASAP 2020 volumetric adsorption analyzer. A high-purity grade (99.999%) of nitrogen gas was used throughout the adsorption experiments. Before the measurements, the freshly prepared samples were activated at 120 °C for 10 h. N₂ adsorption isotherms were measured at 77 K using liquid N₂.

Preparation of the Catalysts. For the CHF-1 catalyst, CHF-1 and BaSO₄ (ratio: 0.33:1) were ground in a ball mill to form a homogeneous mixture. One milligram of the mixture (~2.12 × 10⁻⁴ mmol CHF-1) was used as a catalyst to run the oxidation experiments. For FeTPPCL catalysts, 5 mM stock solutions in DMSO and Tris buffer (v/v 1:1) were prepared and then diluted 200-fold to run the oxidation experiments, whereas for HRP catalyst, 0.024 mM stock solution in deionized water were prepared and then diluted 100-fold to run the oxidation experiments.

ABTS/Pyrogallol Oxidation Reactions and Kinetic Studies. Experiments were carried out using 1.00 mg of CHF-1 catalyst in a reaction volume of 2 mL of Tris buffer solution (0.1 M, pH 5.92) for ABTS or HEPES buffer solution (0.1 M, pH 7.5) for pyrogallol with 1 mM H₂O₂ and in the presence of a series of concentrations of ABTS/pyrogallol (0.01–0.2 mmol/L). Kinetic measurements were carried out in time-course mode by monitoring the absorbance change at 660 nm for ABTS or 420 nm for pyrogallol on a Jasco V550 UV–vis spectrophotometer with 500 rpm at 25 °C. The Michaelis–Menten constant was calculated using the Michaelis–Menten curve fit.

Recycling Experiments of ABTS Oxidation Reaction. The reaction mixture (3.00 mg) was centrifuged for 4 min after the reaction, and the liquid layer was siphoned out. The residual solid was washed with Tris buffer solution and centrifuged. Then, the solid was washed with methanol and centrifuged; this process was repeated twice followed by drying of the solid. Tris buffer solution, H₂O₂, and 0.1 mM ABTS were then added to the UV cell for the next reaction cycle, which was performed under otherwise identical conditions.

■ ASSOCIATED CONTENT

● Supporting Information

IR spectra of monomer and CHF-1; TGA and XRD data and nitrogen adsorption isotherm of CHF-1; and control experiments (PDF). This material is available free of charge via the Internet at <http://pubs.acs.org>.

■ AUTHOR INFORMATION

Corresponding Author

*E-mail: sqma@usf.edu.

Notes

The authors declare no competing financial interest.

■ ACKNOWLEDGMENTS

We acknowledge the University of South Florida for financial support of this work and Dr. Li-June Ming for helpful discussions.

■ REFERENCES

- (1) Tabushi, I. *Coord. Chem. Rev.* **1998**, *86*, 1.
- (2) Wang, Q.; Yang, Z.; Wang, L.; Ma, M.; Xu, B. *Chem. Commun.* **2007**, 1032.
- (3) Feiters, M. C.; Rowan, A. E.; Nolte, R. J. M. *Chem. Soc. Rev.* **2000**, *29*, 375.
- (4) Meunier, B. *Chem. Rev.* **1992**, *92*, 1411.
- (5) McMurry, T.; Groves, J. T. In *Cytochrome P450: Structure, Mechanism, and Biochemistry*; Ortiz de Montellano, P. R., Ed.; Plenum Publishers: New York, 1986.
- (6) Wang, Q.; Yang, Z.; Zhang, X.; Xiao, X.; Chang, C. K.; Xu, B. *Angew. Chem., Int. Ed.* **2007**, *46*, 4285.

- (7) Xue, T.; Jiang, S.; Qu, Y.; Su, Q.; Cheng, R.; Dubin, S.; Chiu, C.-Y.; Kaner, R.; Huang, Y.; Duan, X. *Angew. Chem., Int. Ed.* **2012**, *51*, 3822.

- (8) Shema-Mizrachi, M.; Pavan, G. M.; Levin, E.; Danani, A.; Lemcoff, N. G. *J. Am. Chem. Soc.* **2011**, *133*, 14359.

- (9) Larsen, R. W.; Wojtas, L.; Perman, J.; Musselman, R. L.; Zaworotko, M. J.; Vetromile, C. M. *J. Am. Chem. Soc.* **2011**, *133*, 10356.

- (10) Alkordi, M. H.; Liu, Y.; Larsen, R. W.; Eubank, J. F.; Eddaoudi, M. *J. Am. Chem. Soc.* **2008**, *130*, 12639.

- (11) (a) Lykourinou, V.; Chen, Y.; Wang, X.-S.; Meng, L.; Hoang, T.; Ming, L.-J.; Musselman, R. L.; Ma, S. *J. Am. Chem. Soc.* **2011**, *133*, 10382. (b) Chen, Y.; Lykourinou, V.; Vetromile, C.; Hoang, T.; Ming, L.-J.; Larsen, R.; Ma, S. *J. Am. Chem. Soc.* **2012**, *134*, 13188. (c) Chen, Y.; Lykourinou, V.; Hoang, T.; Ming, L.-J.; Ma, S. *Inorg. Chem.* **2012**, *51*, 9156.

- (12) (a) Zhang, Z.; Zhang, L.; Wojtas, L.; Eddaoudi, M.; Zaworotko, M. J. *J. Am. Chem. Soc.* **2012**, *134*, 928. (b) Li, B.; Zhang, Y.; Ma, D.; Ma, T.; Shi, Z.; Ma, S. *J. Am. Chem. Soc.* **2014**, *136*, 1202.

- (13) (a) Abrahams, B. F.; Hoskins, B. F.; Michail, D. M.; Robson, R. *Nature* **1994**, *369*, 727. (b) Suslick, K. S.; Bhyrappa, P.; Chou, J. H.; Kosal, M. E.; Nakagaki, S.; Smithenry, D. W.; Wilson, S. R. *Acc. Chem. Res.* **2005**, *38*, 283. (c) Goldberg, I. *Chem. Commun.* **2005**, 1243.

- (14) (a) Kosal, M. E.; Chou, J. H.; Wilson, S. R.; Suslick, K. S. *Nat. Mater.* **2002**, *1*, 118. (b) Burnett, B. J.; Barron, P. M.; Hu, C.; Choe, W. *J. Am. Chem. Soc.* **2011**, *133*, 9984. (c) Zou, C.; Zhang, Z.; Xu, X.; Gong, Q.; Li, J.; Wu, C.-D. *J. Am. Chem. Soc.* **2012**, *134*, 87. (d) Shultz, A. M.; Yang, X.-L.; Xie, M.-H.; Zou, C.; He, Y.; Chen, B.; O'Keefe, M.; Wu, C.-D. *J. Am. Chem. Soc.* **2012**, *134*, 10636.

- (15) (a) Wang, X.-S.; Meng, L.; Cheng, Q.; Kim, C.; Wojtas, L.; Chrzanowski, M.; Chen, Y.-S.; Zhang, X. P.; Ma, S. *J. Am. Chem. Soc.* **2011**, *133*, 16322. (b) Wang, X.-S.; Chrzanowski, M.; Kim, C.; Gao, W.-Y.; Wojtas, L.; Cheng, Y.-S.; Zhang, X. P.; Ma, S. *Chem. Commun.* **2012**, *48*, 7173. (c) Wang, X.-S.; Chrzanowski, M.; Gao, W.-Y.; Wojtas, L.; Chen, Y.-S.; Zaworotko, M. J.; Ma, S. *Chem. Sci.* **2012**, *3*, 2823. (d) Meng, L.; Cheng, Q.; Kim, C.; Gao, W.-Y.; Wojtas, L.; Cheng, Y.-S.; Zaworotko, M. J.; Zhang, X. P.; Ma, S. *Angew. Chem., Int. Ed.* **2012**, *10082*. (e) Wang, X.-S.; Chrzanowski, M.; Wojtas, L.; Chen, Y.-S.; Ma, S. *Chem.—Eur. J.* **2013**, *19*, 3297. (f) Gao, W.-Y.; Zhang, Z.; Cash, L.; Wojtas, L.; Chen, Y.-S.; Ma, S. *CrystEngComm* **2013**, *15*, 9320. (g) Gao, W.-Y.; Wojtas, L.; Ma, S. *Chem. Commun.* [Online early access]. DOI: 10.1039/C3CC47542E. Published Online: Nov 27, 2013.

- (16) (a) Farha, O. K.; Hupp, J. T.; Nguyen, S. T. *J. Am. Chem. Soc.* **2009**, *131*, 4204. (b) Farha, O. K.; Shultz, A. M.; Sarjeant, A. A.; Nguyen, S. T.; Hupp, J. T. *J. Am. Chem. Soc.* **2011**, *133*, 5652.

- (17) (a) Bezzu, C. G.; Helliwell, M.; Warren, J. E.; Allan, D. R.; McKeown, N. B. *Science* **2010**, *327*, 1627. (b) Hupp, J. T. *Nat. Chem.* **2010**, *2*, 432.

- (18) Feng, D.; Gu, Z.-Y.; Li, J.-R.; Jiang, H.-L.; Wei, Z.; Zhou, H.-C. *Angew. Chem., Int. Ed.* **2012**, *51*, 10307.

- (19) (a) Chen, Y.; Tran, H.; Ma, S. *Inorg. Chem.* **2012**, *51*, 12600. (b) Morris, W.; Voloskiy, B.; Demir, S.; Gándara, F.; McGrier, P. L.; Furukawa, H.; Cascio, D.; Stoddart, J. F.; Yaghi, O. M. *Inorg. Chem.* **2012**, *51*, 6443.

- (20) (a) Kitagawa, S.; Kitaura, R.; Noro, S.-I. *Angew. Chem., Int. Ed.* **2004**, *43*, 2334. (b) Zhou, H.-C.; Long, J. R.; Yaghi, O. M. *Chem. Rev.* **2012**, *112*, 673. (c) Furukawa, H.; Cordova, K. E.; O'Keefe, M.; Yaghi, O. M. *Science* **2013**, *341*, 974.

- (21) (a) Ma, S.; Zhou, H.-C. *Chem. Commun.* **2010**, *46*, 44. (b) Suh, M. P.; Park, H. J.; Prasad, T. K.; Lim, D.-W. *Chem. Rev.* **2012**, *112*, 782. (c) Wu, H.; Gong, Q.; Olson, D. H.; Li, J. *Chem. Rev.* **2012**, *112*, 836.

- (22) (a) Li, J.-R.; Kuppler, R. J.; Zhou, H.-C. *Chem. Soc. Rev.* **2009**, *38*, 1477. (b) Ma, S.; Meng, L. *Pure Appl. Chem.* **2011**, *83*, 167. (c) Li, J.-R.; Sculley, J.; Zhou, H.-C. *Chem. Rev.* **2012**, *112*, 869.

- (23) (a) D'Alessandro, D. M.; Smit, B.; Long, J. R. *Angew. Chem., Int. Ed.* **2010**, *49*, 6058. (b) Li, J.-R.; Ma, Y.; McCarthy, M. C.; Sculley, J.; Yu, J.; Jeong, H.-K.; Balbuena, P. B.; Zhou, H.-C. *Coord. Chem. Rev.* **2011**, *255*, 1791. (c) Liu, J.; Thallapally, P. K.; McGrail, B. P.; Brown,

- D. R.; Liu, J. *Chem. Soc. Rev.* **2012**, *41*, 2308. (d) Nugent, P.; Belmabkhout, Y.; Burd, S. D.; Cairns, A. J.; Luebke, R.; Forrest, K.; Pham, T.; Ma, S.; Space, B.; Wojtas, L.; Eddaoudi, M.; Zaworotko, M. *J. Nature* **2013**, *495*, 80.
- (24) (a) Lee, J.; Farha, O. K.; Roberts, J.; Scheidt, K. A.; Nguyen, S. T.; Hupp, J. T. *Chem. Soc. Rev.* **2009**, *38*, 1450. (b) Ma, L. Q.; Abney, C.; Lin, W. B. *Chem. Soc. Rev.* **2009**, *38*, 1248. (c) Corma, A.; Garcia, H.; Llabrés i Xamena, F. X. *Chem. Rev.* **2010**, *110*, 4606. (d) Yoon, M.; Srirambalaji, R.; Kim, K. *Chem. Rev.* **2012**, *112*, 1196. (e) Gao, W.-Y.; Chen, Y.; Niu, Y.; Williams, K.; Cash, L.; Perez, P. J.; Wojtas, L.; Cai, J.; Chen, Y.-S.; Ma, S. *Angew Chem., Int. Ed.* [Online early access]. DOI: 10.1002/anie.201309778. Published Online: Feb 4, **2014**.
- (25) (a) Sumida, K.; Rogow, D. L.; Mason, J. A.; McDonald, T. M.; Bloch, E. D.; Herm, Z. R.; Bae, T.-H.; Long, J. R. *Chem. Rev.* **2012**, *112*, 724. (b) Cychosz, K. A.; Matzger, A. J. *Langmuir* **2010**, *26*, 17198. (c) Colombo, V.; Galli, S.; Choi, H. J.; Han, G. D.; Maspero, A.; Palmisano, G.; Masciocchi, N.; Long, J. R. *Chem. Sci.* **2011**, *2*, 1311.
- (26) (a) Cote, A. P.; Benin, A. I.; Ockwig, N. W.; O'Keeffe, M.; Matzger, A. J.; Yaghi, O. M. *Science* **2005**, *310*, 1166. (b) El-Kaderi, H. M.; Hunt, J. R.; Mendoza-Cortes, J. L.; Cote, A. P.; Taylor, R. E.; O'Keeffe, M.; Yaghi, O. M. *Science* **2007**, *316*, 268. (c) Mastalerz, M. *Angew. Chem., Int. Ed.* **2008**, *47*, 445. (d) Zwaneveld, N. A. A.; Pawlak, R.; Abel, M.; Catalin, D.; Gimes, D.; Bertin, D.; Porte, L. *J. Am. Chem. Soc.* **2008**, *130*, 6678. (e) Spitler, E. L.; Dichtel, W. R. *Nat. Chem.* **2010**, *2*, 672. (f) Lanni, L. M.; Tilford, R. W.; Bharathy, M.; Lavigne, J. *J. Am. Chem. Soc.* **2011**, *133*, 13975.
- (27) Cooper, A. I. *Adv. Mater.* **2009**, *21*, 1291.
- (28) Xu, Y.; Jin, S.; Xu, H.; Nagai, A.; Jiang, D. *Chem. Soc. Rev.* **2013**, *42*, 8012.
- (29) Xie, Y.; Wang, T.-T.; Liu, X.-H.; Zou, K.; Deng, W.-Q. *Nat. Commun.* **2013**, *4*, 1960.
- (30) Ben, T.; Ren, H.; Ma, S.; Cao, D.; Lan, J.; Jing, X.; Wang, W.; Xu, J.; Deng, F.; Simmons, J. M.; Qiu, S.; Zhu, G. *Angew. Chem., Int. Ed.* **2009**, *48*, 9457.
- (31) (a) Lu, W.; Yuan, D.; Zhao, D.; Schilling, C. I.; Plietzsch, O.; Muller, T.; Brase, S.; Guenther, J.; Blumel, J.; Krishna, R.; Li, Z.; Zhou, H.-C. *Chem. Mater.* **2010**, *22*, 5964. (b) Yuan, D.; Lu, W.; Zhao, D.; Zhou, H.-C. *Adv. Mater.* **2011**, *23*, 3723.
- (32) Wang, X.-S.; Liu, J.; Bonefont, J. M.; Yuan, D.-Q.; Thallapally, P. K.; Ma, S. *Chem. Commun.* **2013**, *49*, 1533.
- (33) Zhu, X.; Tian, C.; Mahurin, S. M.; Chai, S.-H.; Wang, C.; Brown, S.; Veith, G. M.; Luo, H.; Liu, H.; Dai, S. *J. Am. Chem. Soc.* **2012**, *134*, 104784.
- (34) Patel, H. A.; Hyun, J. S.; Park, J.; Chen, D. P.; Jung, Y.; Yavuz, C. T.; Coskun, A. *Nat. Commun.* **2013**, *4*, 1357.
- (35) Nagai, A.; Guo, Z.; Feng, X.; Jin, S.; Chen, X.; Ding, X.; Jiang, D. *Nat. Commun.* **2011**, *2*, 1542.
- (36) Zou, X.; Ren, H.; Zhu, G. *Chem. Commun.* **2013**, *49*, 3925.
- (37) Ding, S.-Y.; Gao, J.; Wang, Q.; Zhang, Y.; Song, W.-G.; Su, C.-Y.; Wang, W. *J. Am. Chem. Soc.* **2011**, *133*, 19816.
- (38) Thomas, A. *Angew. Chem., Int. Ed.* **2010**, *49*, 8328.
- (39) Konstas, K.; Taylor, J. W.; Thornton, A. W.; Doherty, C. M.; Lim, W. X.; Bastow, T. J.; Kennedy, D. F.; Wood, C. D.; Cox, B. J.; Hill, J. M.; Hill, A. J.; Hill, M. R. *Angew. Chem., Int. Ed.* **2012**, *51*, 6639.
- (40) McKeown, N. B.; Budd, P. M. *Chem. Soc. Rev.* **2006**, *35*, 675.
- (41) Wood, C. D.; Tan, B.; Trewin, A.; Su, F.; Rosseinsky, M. J.; Bradshaw, D.; Sun, Y.; Zhou, L.; Cooper, A. I. *Adv. Mater.* **2008**, *20*, 1916.
- (42) Rabbani, M. G.; Sekizkardes, A. K.; El-Kadri, O. M.; Kaafarani, B. R.; El-Kaderi, H. M. *J. Mater. Chem.* **2012**, *22*, 25409.
- (43) Kou, Y.; Xu, Y.; Guo, Z.; Jiang, D. *Angew. Chem., Int. Ed.* **2011**, *50*, 8753.
- (44) Zhu, Y.; Long, H.; Zhang, W. *Chem. Mater.* **2013**, *25*, 1630.
- (45) (a) Chen, L.; Yang, Y.; Jiang, D. *J. Am. Chem. Soc.* **2010**, *132*, 9138. (b) Chen, L.; Yang, Y.; Guo, Z.; Jiang, D. *Adv. Mater.* **2011**, *23*, 3149.
- (46) Shultz, A. M.; Farha, O. K.; Hupp, J. T.; Nguyen, S. T. *Chem. Sci.* **2011**, *2*, 686.
- (47) Mackintosh, H. J.; Budd, P. M.; McKeown, N. B. *J. Mater. Chem.* **2008**, *18*, 573.
- (48) Zhang, Y.; Riduan, S. N. *Chem. Soc. Rev.* **2012**, *41*, 2083.
- (49) *Accelrys Materials Studio*, release 5.0; Accelrys Software, Inc.: San Diego, CA, 2008.